GEOPHYSICS, VOL. 81, NO. 4 (JULY-AUGUST 2016); P. 1–9, 13 FIGS.
10.1190/GEO2015-0474.1

Interpretation of magnetic resonance measurements in the varying earth's magnetic field

Anatoly Legchenko[1], Jean-Michel Vouillamoz[1], Fabrice Messan Amene Lawson[2], Christian Alle[2], Marc Descloitres[1], and Marie Boucher[1]

ABSTRACT

At the scale of a magnetic resonance sounding (MRS) field setup, the earth's magnetic field in the subsurface may vary laterally with depth and over time. These variations can be caused by different natural factors and generally cannot be compensated for by accurate tuning of the measuring device. The varying geomagnetic field (GMF) causes nonresonance conditions of excitation that affect the amplitude and phase of the MRS signal. Usually, variations of the GMF do not exceed a few hertz and their effect on the amplitude is relatively small, permitting us to assume near-resonance conditions for inversion. However, in some cases, the results may be erroneous if a varying GMF is not taken into account. Motivated by possible improvements in MRS inversion, we have developed a procedure for measuring and interpreting MRS data that considers a varying GMF. Our results showed that it is relatively easy to take a time-varying GMF into account. As a demonstration, we have developed the inversion of MRS data measured in Benin (West Africa). A depth-varying GMF is a more complex problem, and to consider this, we have developed an algorithm of nonlinear inversion. We have tested this approach on synthetic data, which resulted in an improved inversion. Field validation of this procedure awaits the discovery of a suitable test site with known variations of the earth's magnetic field in the subsurface.

INTRODUCTION

Magnetic resonance sounding (MRS) measurements are performed in the earth's magnetic field, which acts as a static magnetic field and is usually assumed to be constant for a given area. A constant geomagnetic field (GMF) allows setting a frequency of the excitation pulse close to the resonance frequency of protons in the GMF (Larmor frequency), thus carrying out MRS measurements under near-resonance conditions. In practice, the excitation frequency may be set a few hertz off resonance for creating an off-resonance excitation. An offset of a few hertz between the excitation and the Larmor frequencies is commonly considered as being of relatively small importance, and in most cases, the frequency offset is either neglected, or a constant frequency offset is used. These assumptions may be justified for amplitude inversion, but the MRS signal phase is more sensitive to frequency offset. Thus, neglecting the off-resonance excitation is less easily justified for the inversion of complex signals that require accurate measuring and forward modeling of the MRS response (Legchenko, 2004; Walbrecker et al., 2011).

Meanwhile, it was reported that inversion of complex signals could help in the interpretation of MRS data: The inversion of complex signals for water content provides a better resolution (Weichman et al., 2002; Braun et al., 2005) and can give better results in the inversion for resistivity distribution (Braun and Yaramanci, 2008). Accurate tuning of the MRS system to the Larmor frequency is not always possible because GMF values are not always constant. Depending on the magnetic properties of surrounding rocks, the GMF may be perturbed locally at the pore-size scale (Roy et al., 2008), or it can gradually change its intensity laterally and with depth (Legchenko et al., 2010). The earth's magnetic field may also vary during measuring time (Vouillamoz et al., 2008). GMF variations modify the Larmor frequency, creating off-resonance excitation

Manuscript received by the Editor 4 September 2015; revised manuscript received 2 January 2016.
[1]IRD/UJF-Grenoble 1/CNRS/G-INP, LTHE UMR 5564, Grenoble, France. E-mail: Anatoli.Legtchenko@ird.fr; jean-michel.vouillamoz@ird.fr; marc.descloitres@ird.fr; Marie.Boucher@ird.fr.
[2]University of Abomey Calavi, Cotonou, Bénin. E-mail: lawson.amen@yahoo.fr; christian.alle@ird.fr.

conditions, and thus affecting magnetic resonance signals (Legchenko et al., 1997; Legchenko, 2004; Hertrich, 2008).

Motivated by possible improvements of MRS inversion, we developed and successfully tested on synthetic and real data, a procedure of measuring and interpretation of MRS data that takes into account time and depth variations of the earth's magnetic field. In this paper, we report the results of our study.

BACKGROUND

An MRS field setup consists of a wire loop on the surface energized by an alternating-current pulse $i(t) = I_0 \cos(\omega t)$. The current frequency ω is set close to the Larmor frequency of the protons ω_0 in the earth's magnetic field B_0. Thus

$$\omega \approx \omega_0 = 2\pi f_0 = \gamma B_0, \tag{1}$$

where γ is the gyromagnetic ratio. Under exact resonance, the frequency offset between the Larmor frequency and the excitation frequency is equal to zero

$$\Delta\omega = \omega_0 - \omega = 0, \tag{2}$$

but in practice, GMF may vary, thus creating a frequency offset $\Delta\omega = \gamma(B_0 + \Delta B) - \omega \neq 0$.

For computing the MRS signal, we assume one coincident transmitting/receiving loop (T_x/R_x). Performing free induction decay measurements with one current pulse (FID1), the received signal decaying with the relaxation time T_2^* can be computed as

$$e(q,t) = I_0^{-1} \int_V \omega_0 B_1 e^{2j\varphi_0^{Tx}} M_\perp e^{\varphi_{\Delta\omega}} w(\mathbf{r}) e^{-t/T_2^*(\mathbf{r})} \times e^{j\omega_0 t} dV, \tag{3}$$

where $w(\mathbf{r})$ is the water-content distribution. The component of the loop magnetic field perpendicular to the earth's magnetic field B_1 causes rotation of the magnetic moments of protons at the flip angle θ, which depends on the pulse moment $q = I_0\tau$, with I_0 and τ being the amplitude and duration of the pulse, respectively; φ_0^{Tx} is the phase shift caused by electrically conductive subsurface $\rho(\mathbf{r})$ and $\varphi_{\Delta\omega}$ is the phase shift caused by the off-resonance conditions of excitation (Legchenko, 2004); $M_\perp$ is the transverse component of the nuclear magnetization computed after Mansfield et al. (1979):

$$M_\perp^2 = M_x^2 + M_y^2, \tag{4}$$

where

$$\begin{cases} M_x = \frac{\omega_1 \Delta\omega}{\omega_{\text{eff}}^2}(1 - \cos(\omega_{\text{eff}}\tau))M_0, \\ M_y = \frac{\omega_1}{\omega_{\text{eff}}}\sin(\omega_{\text{eff}}\tau)M_0, \\ M_z = \frac{\Delta\omega^2 + \omega_1^2 \cos(\omega_{\text{eff}}\tau)}{\omega_{\text{eff}}^2} M_0. \end{cases} \tag{5}$$

In equation 5, M_0 is the macroscopic spin magnetization, $\omega_{\text{eff}}^2 = \omega_1^2 + \Delta\omega^2$, and $\omega_1 = 0.5\gamma B_1$. The M_x component corresponds to the imaginary part of the MRS signal and M_y to its real part. If $\Delta\omega = 0$, then $M_x = 0$ and the signal is real. Otherwise it is complex.

In integral equation 3, $e(q,t)$ is a set of experimental data and the unknown functions of interest are: water content $w(\mathbf{r})$, electrical resistivity of the subsurface $\rho(\mathbf{r})$, the Larmor frequency $\omega_0(\mathbf{r})$ closely related to the earth's magnetic field, and relaxation time $T_2^*(\mathbf{r})$.

FORWARD MODELING

Legchenko and Valla (2002) show that the amplitude of the MRS signal is a square function of the earth's magnetic field (in equation 1, ω_0 and M_0 are proportional to B_0). Let us estimate the influence of GMF magnitude on the signal amplitude. Considering a 10 Hz increase in GMF relative to the Larmor frequency of 2000 Hz, we obtain an approximately 1% higher signal of 2010 Hz, which can be ignored in practice. However, under off-resonance excitation, the MRS signal becomes complex and GMF variations have a larger effect on the MRS signal. For modeling, we use equations 1 and 5 and assume a 100×100 m square loop, 100 ohm-m half-space, water content $w = 20\%$, and we neglect relaxation. We use the earth's magnetic field typical for Europe (inclination of 55°N and a Larmor frequency of 2000 Hz).

First, we demonstrated the influence of off-resonance excitation by applying a constant frequency offset. Figures 1 and 2 show the MRS (a) amplitude and (b) phase computed under near-resonance conditions, and considering ±5 Hz frequency offset. It is seen that the amplitude and phase depend on the frequency offset and that these effects are different for shallow and deep layers.

Then, we assumed a varying GMF and used one thick water-saturated layer from 0 to 100 m ($w = 20\%$). Two cases were studied: (1) the frequency offset varies linearly from 0 to 100 m depth and (2) the frequency offset varies linearly from the first to the last pulse moment, which may correspond to a time-varying GMF (considering $\omega_0(t) \rightarrow \omega_0(q)$). The correspondence between $\omega_0(t)$ and $\omega_0(q)$ depends on the measuring sequence used for data acquisition. The simplest way of measuring consists of progressively increasing the pulse moment. In this case, $\omega_0(t)$

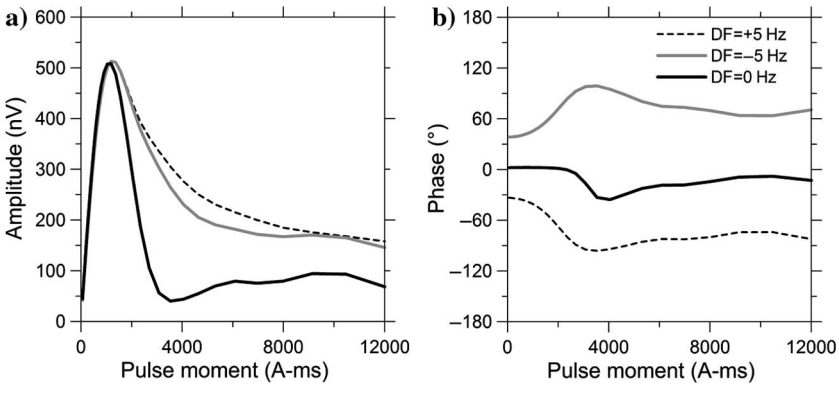

Figure 1. (a) Initial amplitude and (b) phase of MRS response computed considering one water-saturated layer located between 10 and 20 m ($w = 20\%$). Three cases are presented: near resonance (black line), a frequency offset of +5 Hz (dashed line), and a frequency offset of −5 Hz (gray line).

and $\omega_0(q)$ are linked through the time needed for the stacking of each pulse moment. Another measuring procedure consists of discharging the storage capacity of the generator by a series of pulses, thus progressively decreasing the current amplitude in the loop for each pulse. Note that, if GMF varies during measuring time, this procedure may cause stacking signals measured with different frequency offsets, thereby introducing additional difficulties for interpretation. In this case, information about a time-varying GMF may be lost. In practice, available MRS instruments allow easy programming of the measuring procedure and one can easily use any other pulse sequence.

When assuming a time-varying GMF, the MRS response $e(q)$ is computed using the same Larmor frequency value $\omega_0(q)$ for all depths $z_j(q = q_i, i = 1,2, \ldots, I)$. However, for a depth-varying GMF, the Larmor frequency $\omega_0(z)$ is a function of depth for all pulse moments $q_i(z = z_j, j = 1,2, \ldots, J)$. Figures 3 and 4 show (a) amplitude and (b) phase of the computed MRS signal considering a linearly increasing Larmor frequency (from 2000 to 2010 Hz) and a linearly decreasing Larmor frequency (from 2010 to 2000 Hz), respectively. One sees that amplitude and phase of the signal depend on the GMF variations and the water-content distribution. Figure 5 shows the MRS signal frequency versus pulse moment for the models shown in Figures 3 and 4; these frequencies correspond to the maximum of spectra for each pulse moment. Depending on the origin of the GMF variation and on the water-content distribution, the frequencies may be difficult to resolve even when using an inversion procedure.

It is possible that both effects are present, with GMF varying over time and with depth. This requires carrying out a nonlinear inversion for $\omega_0(z)$ considering a time-varying GMF in the forward-modeling routine. Such a mixed case can be identified by jointly using different techniques:

1) A depth-varying GMF can be identified by the existence of a spin-echo (SE) signal, which points to a heterogeneous GMF even when an FID signal is observed (Vouillamoz et al., 2011).
2) Surface monitoring of the GMF with a magnetometer, or repetitive measurements of one or two pulse-moment values will allow detecting a time-varying GMF.

The problem may be even more complex, where a lateral variation of the GMF occurs inside measuring loop (vertical magnetic dykes, for example). Such a case may require 3D measuring and inversion procedures. The use of MRS under these complex conditions is beyond the scope of our paper.

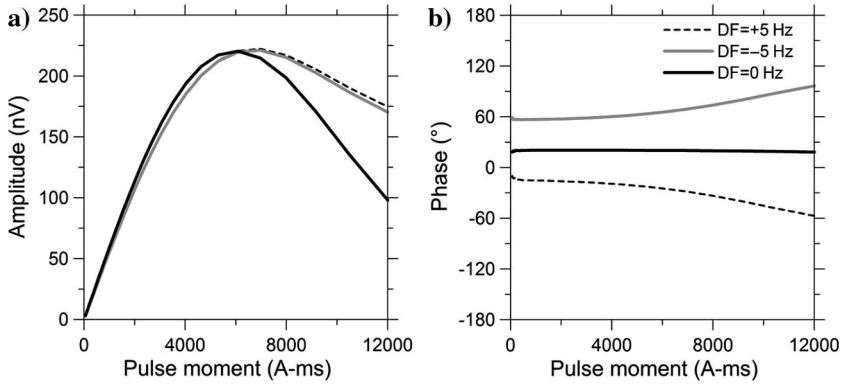

Figure 2. (a) Initial amplitude and (b) phase of MRS response computed considering one water-saturated layer located between 50 and 60 m ($w = 20\%$). Three cases are presented: near resonance (black line), frequency offset of +5 Hz (dashed line), and a frequency offset of −5 Hz (gray line).

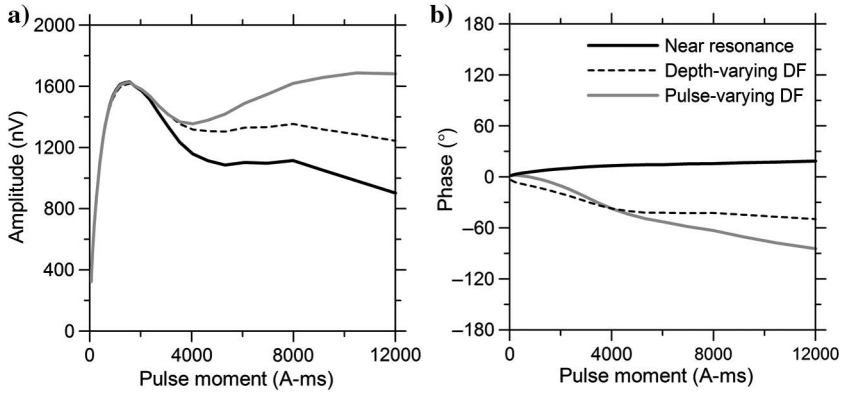

Figure 3. (a) Initial amplitude and (b) phase of MRS response computed considering one water-saturated layer between 0 and 100 m ($w = 20\%$). Three cases are presented: near resonance (black line), a depth-varying frequency offset between 0 and +10 Hz (dashed line), and a pulse-moment varying frequency offset also between 0 and +10 Hz (gray line).

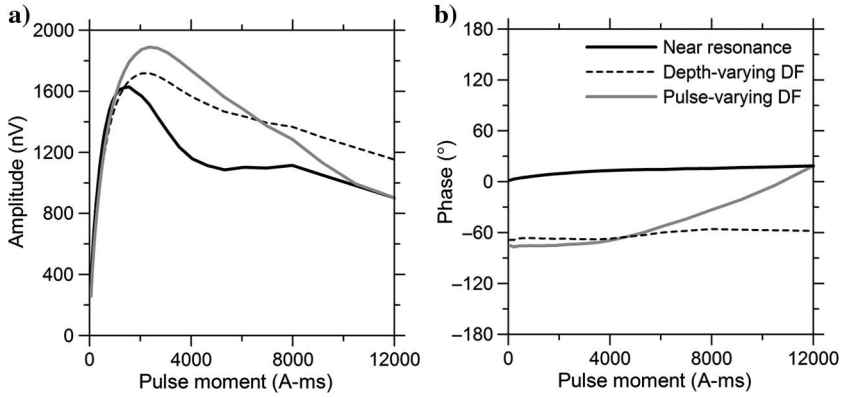

Figure 4. (a) Initial amplitude and (b) phase of MRS response computed considering one water-saturated layer between 0 and 100 m ($w = 20\%$). Three cases are presented: near resonance (black line), depth-varying frequency offset between +10 and 0 Hz (dashed line), and pulse-moment varying frequency offset also between +10 and +0 Hz (gray line).

THE INVERSION ALGORITHM

Resolution of equation 3 can be straightforward when using a global nonlinear inversion. However, we found that such an approach requires data with a high signal-to-noise ratio (S/N) and may be computationally difficult. For simplifying, the inversion we did the following:

1) It is shown by Braun and Yaramanci (2008) that the resistivity $\rho(\mathbf{r})$ can be resolved from inversion of an MRS data set. However, the resistivity can also be measured by one of the well-developed geophysical methods that provide better resolution than MRS inversion (Vouillamoz et al., 2002, 2003; Behroozmand et al., 2012). For example, the uncertainty in the results provided by the time-domain electromagnetic method has a limited influence on MRS inversion for water content (Legchenko et al., 2008). Thus, in equation 3, we assume $\rho(z)$ to be known from other measurements.

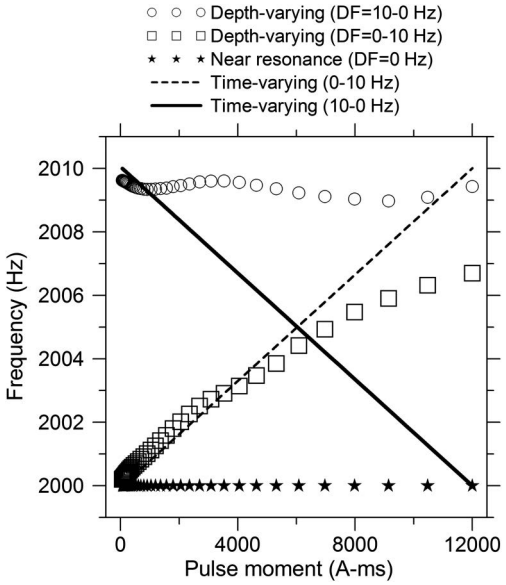

Figure 5. Frequency of the MRS signal versus pulse moment computed considering models of increasing and decreasing GMFs presented in Figures 3 and 4, respectively.

2) Our algorithm is split into two parts: (1) a linear inversion for the water content $w(z)$ and (2) a nonlinear inversion for the Larmor frequency $\omega_0(z)$. Both parts are linked by an iterative procedure presented in Figure 6. For the linear inversion, equation 3 is approximated by the matrix equation $\mathbf{Aw} = \mathbf{e}$, and then resolved using the Tikhonov regularization method (Legchenko and Shushakov, 1998). For computing matrix $\mathbf{A}$, we use either the measured distribution of the Larmor frequency $\omega_0(q)$ (for time-varying GMF), or the $\omega_0(z)$ value that was iteratively derived from the nonlinear inversion (for depth-varying GMF). Nonlinear inversion uses a nonlinear least-square optimization (Marquardt, 1963). The water content $w(z)$ for the forward model is provided by the linear inversion. When performing an inversion for $\omega_0(z)$, we assume an average Larmor frequency value for each value of the pulse moment, thus transforming the recorded time series into an $\omega_0(q)$ data set using the Fourier transform. Spectra of MRS signals can be rather complex. Signals with close frequencies, as well as with short relaxation times cause broadening MRS spectra, thus creating equivalence between frequency and relaxation time. In this paper, we do not consider an easy case of well-separated Larmor frequencies of long signals (frequency offset abs$(\Delta\omega) > 5/2\pi$ Hz and $T_2^* > 200$ ms). Accurate resolution of these frequencies is not easy and requires a high S/N. However, MRS inversion is relatively insensitive to small variations of the Larmor frequency and, for simplifying our algorithm, we used only the maximum of the MRS spectra for frequency estimates of each pulse moment. The inversion algorithm is the same for a depth-varying and a time-varying GMF. However, although for depth-varying GMF, the frequency variation $\omega_0(z)$ is derived from a nonlinear inversion, in the time-varying GMF, $\omega_0(q)$ is directly provided by frequency measurements. This allows skipping the nonlinear inversion procedure, using $\omega_0(q) \pm \varepsilon_\omega$ for better adjustment of the phase fit. Inversion stops when the residual between experimental and measured data, computed with individual weights for frequency, amplitude, and phase (P_ω, P_e, and P_φ), becomes smaller than the noise level. To avoid infinite loops when the noise estimates are too optimistic and corresponding accuracy cannot be attained, the inversion procedure is further limited by a maximum number of iterations.

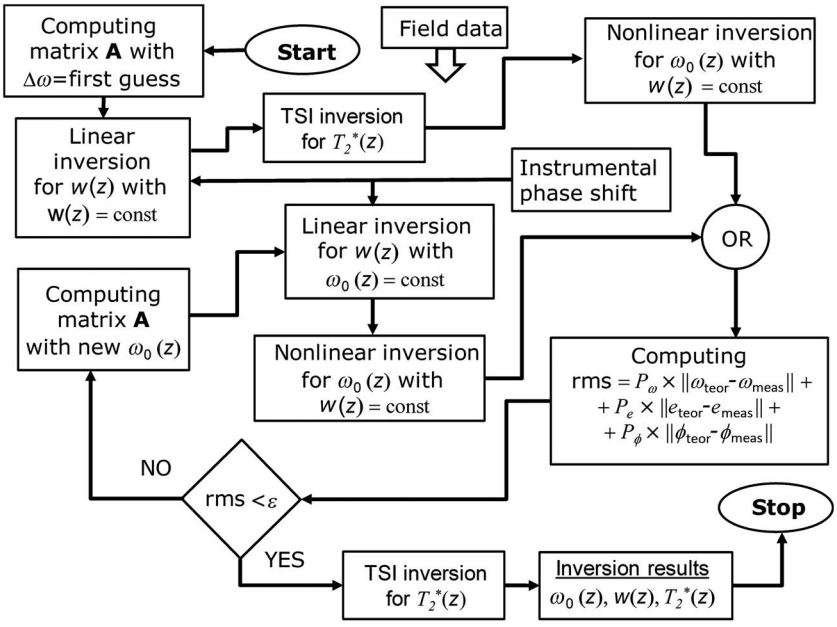

Figure 6. Flowchart of the inversion algorithm adapted to a depth-varying GMF.

3) Inversion is carried out using complex MRS signals (amplitude and phase). The noise level is estimated for real and imagi-

nary parts (and thus for the amplitude), using records obtained before the pulse. The weights are set as an inverse of the noise standard deviation, from (a) standard deviation of the amplitude ($P_e = 1/\sigma_{Ne}$), and (b) the sum of standard deviations for real and imaginary parts of the signal for the phase ($P_\varphi = (1/[\sigma_{\mathrm{Re}(N)} + \sigma_{\mathrm{Im}(N)}])$). The frequency weight ($P_\omega = 1/\varepsilon_{N\omega}$) is set as an inverse of the measuring uncertainty, which is estimated as the root-mean-square error between the measured frequency of the MRS signal and the second-order polynomial fit of this measured frequency.

Inversion routine allows modifying the weights manually, considering the following points:

1) Amplitude is the most reliable parameter with the highest weight (a good fit of the amplitude data must always be respected).
2) However, when measuring in complex geology (magnetic rocks, very heterogeneous subsurface, etc.), the accuracy of the forward modeling of phase and frequency may be limited. Consequently, their weights can be set smaller than that for the amplitude.
3) Different inversion schemes for the relaxation time $T_2^*(z)$ can be found in the literature (Mohnke and Yaramanci, 2002, 2005; Mueller-Petke and Yaramanci, 2010). We use the time-step-inversion, which consists of series of inversions for water content corresponding to shifted time steps and a following exponential smoothing of the water content $w_j(t)$ for each depth z_j (Legchenko and Valla, 2002).

Practical implementation of the above-described inversion algorithm did not reveal significant mathematical difficulties and convergence was reasonably rapid. The linear inversion is very fast (a few seconds for 80 iterations), but the nonlinear inversion requires volume integration and hence inversion is longer (30–60 s for each iteration). Thus, inversion time largely depends on the time necessary for computing the matrix **A**. Faster convergence inversion for the Larmor frequency in depth-varying GMF requires a good S/N and a reasonably good first guess. With our data sets, it was sufficient to compute the matrix **A** less than 10 times. A large equivalence between time and depth variations of the earth's magnetic field, and thus of the frequency offset, requires knowledge of the cause of the Larmor frequency variations.

EXAMPLES OF APPLICATION

Synthetic data set

For demonstration of the nonlinear inversion scheme, we used a synthetic data set computed by assuming one water-saturated layer ($w = 20\%$, $T_2^* = 200$ ms) located between 30 and 60 m (dashed gray line in Figure 7). The depth-varying GMF creates a frequency offset DF that linearly changes from 0 to 10 Hz in the depth interval between 30 and 60 m. For modeling, we used a 100 × 100 m square loop, a 100 ohm-m half-space, the earth's magnetic field with an inclination of 55°N, and a Larmor frequency of 2000 Hz. A normally distributed synthetic noise with a mean of 10 nV was added to the computed signals.

For inversion of this data set, we present three different approaches:

1) The forward model for inversion is computed using the frequency offset that corresponds to the initial model. Inversion with this "true" frequency offset shows how well these data can be resolved, assuming a correct value of the frequency offset. In Figure 7, this inverse model is shown by a dashed black line.
2) The forward model for inversion is computed using the frequency offset derived from the nonlinear inversion of the frequency offset. In Figure 7, this inverse model is shown by a solid black line, demonstrating the efficiency of the newly developed inversion scheme.
3) The forward model for inversion is computed assuming a time-varying frequency offset $DF(q)$ that is equal to the frequency offset computed with the initial model with depth-varying frequency offset (conversion is done for $DF(z) \rightarrow DF(q)$). In Figure 7, this inverse model is shown by a solid gray line. This example is presented for demonstration of the possible errors in the inverse model caused by an erroneous determination of the origin of GMF variations.

Figure 7 shows that our inversion scheme allows a correct reconstruction of the depth-varying frequency offset and provides a $w(z)$ similar to that obtained with the "true" GMF model, thus confirming the feasibility of the inversion procedure. The synthetic data and inversion fits of Figure 8 suggest that inversion was correct and that all the inverse models in Figure 7 are equivalent. Inversion carried out with an intentionally erroneous origin of GMF variations (time-varying instead of depth-varying DF) provides a less accurate inverse model, thus demonstrating the importance of correct determination of the GMF variations.

In practice, the uncertainty of the frequency forward modeling necessary for inversion is composed of two major parts: measuring inaccuracy (less than ±0.2 Hz for measurements with a high S/N and not more than ±0.5 Hz for a typical MRS sounding) and forward modeling inaccuracy. The latter depends upon the complexity

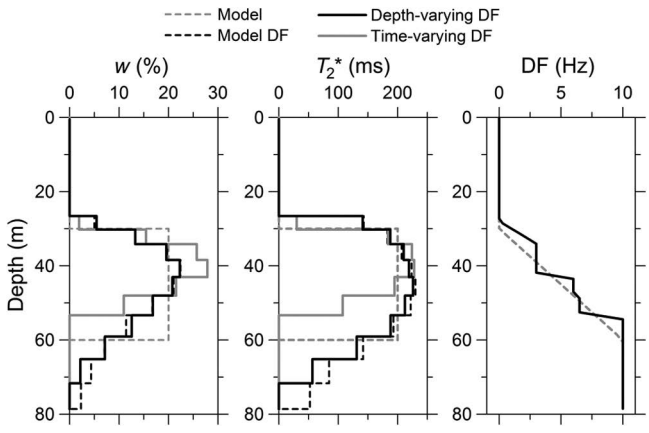

Figure 7. Inversion of a synthetic data set computed assuming the depth-varying frequency offset (initial model, dashed gray line). Inverse models were obtained considering the true frequency offset given by the forward model (dashed black line) and frequency offset provided by the nonlinear inversion (solid black line). For comparison, an inversion made by assuming an intentionally erroneous time-varying frequency offset instead of the depth-varying one, is also presented (solid gray line). The time-varying frequency offset was set such that the variation of the frequency offset $DF(q)$ is equal for both cases.

of the subsurface and cannot be easily estimated because the subsurface is not well known at the scale of an MRS loop.

Numerical modeling suggests that a ±1 Hz error does not cause large errors in inversion. For example, Figure 7 shows variations in the inversion results computed for a 10 Hz frequency offset. Thus, a 0.5–1 Hz uncertainty in the frequency-offset estimate may cause variations in the inversion results that are smaller than the inversion uncertainty caused by the equivalence problem.

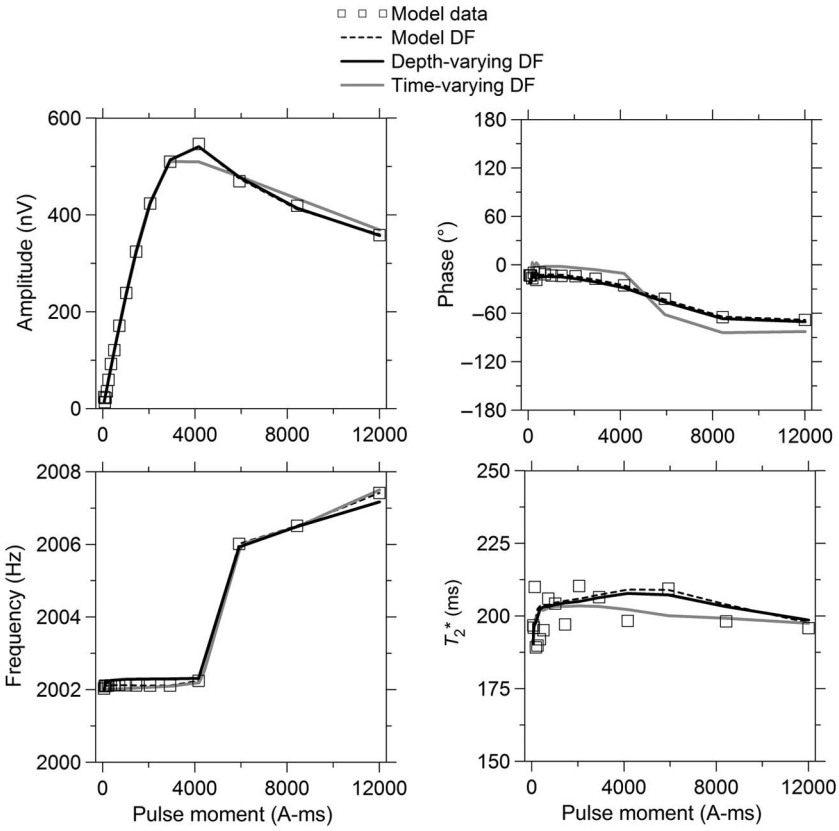

Figure 8. Synthetic data set and inversion fit corresponding to the inverse models are shown in Figure 7. Note that the inverse models computed with the depth-varying frequency offset derived from nonlinear inversion and the frequency offset set in the initial model produce very similar signals that are barely distinguishable in the graphs.

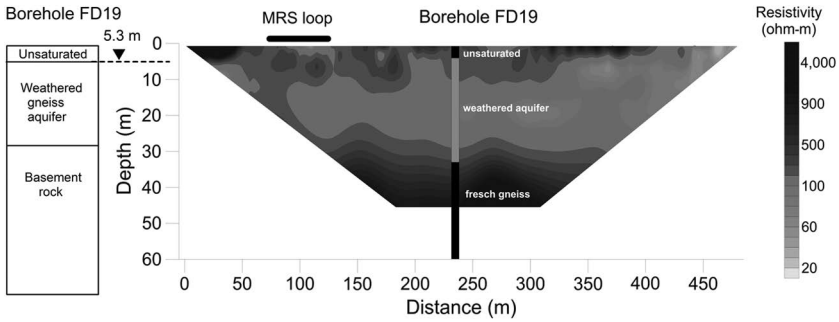

Figure 9. ERT and borehole results in Benin. A weathered gneiss aquifer located between 5.3 and 30 m is clearly delineated on the ERT profile by lower electrical resistivity. AT lower than 30 m, the resistivity is >1000 ohm-m. The MRS loop was located within the ERT profile at a distance between 70 and 120 m and the boreholes at a distance of 178 m.

Real data set

MRS was used for investigating groundwater resources in Benin, carried out as part of the GRIBA project (EuropeAid program). The subsurface of the investigated site is composed of hard rock (mainly gneiss) that is weathered down to approximately 30 to 35 m. A borehole drilled in the area shows that this weathered part contains an aquifer down to approximately 30 m with a static water level at 5.3 m. The electrical resistivity tomography (ERT) profile and the borehole log (Figure 9) indicate a weathered-rock formation well resolved by ERT due to lower electrical resistivity compared with the underlying hard rock (>600 ohm-m). The MRS station is located in the area corresponding to the distance between 70 and 120 m along the profile. For the MRS survey, we used the NUMIS^{plus} system with a 50 × 50 m square loop (two turns). The Larmor frequency was approximately 1415 Hz. ERT results suggest a four-layer geoelectrical model: 250 ohm-m between 0 and 12 m, 150 ohm-m between 12 and 27 m, 600 ohm-m between 27 and 38 m, and 1000 ohm-m less than 38 m.

The earth's magnetic field was monitored with a proton magnetometer on the surface near the MRS loop. The measurements showed particularly pronounced variations in the GMF toward noon. Figure 10a shows examples of the GMF drift observed in 2012 and in 2014. Corresponding measurements of the MRS signal frequency versus pulse moment, carried out with the MRS instrument, are shown in Figure 10b. Figure 10c shows correspondence between the pulse moment and daytime of realization of each pulse, which allows conversion $\omega_0(t) \rightarrow \omega_0(q)$. The regularity of measuring with progressively increasing pulse moment was intentionally perturbed for four largest pulses. This perturbation caused the difference in the Larmor frequency for corresponding pulses between that measured with a proton magnetometer and the MRS instrument (Figure 10a and 10b). These observations confirm that we are dealing with a time-varying earth's magnetic field. To verify additionally possible depth variations in the GMF, we carried out SE experiments. The observed absence of SE corroborates the geology composed of nonmagnetic gneiss. The relaxation times estimated as $T_2^* \approx$ 180 ms and $T_1 \approx 450$ ms further suggest a homogeneous GMF. These observations allowed selecting a model with a time-varying frequency offset and shallow-water correction (Legchenko, 2013). For inversion, we used discretization based on singular values decomposition (SVD) with subsequent Tikhonov regularization. The uncertainty and resolution in the inverse model were computed through the 95% confidence interval and the resolution matrix provided by SVD (Legchenko and Pierrat, 2014).

Inversion of the complex signals shows that the aquifer was well resolved (Figure 11), and

the MRS inverse model is in a good agreement with the ERT and borehole data. However, if we neglect varying frequency offset and assume near-resonance conditions for inversion, then the phase cannot be correctly computed and inversion has to be carried out using only amplitudes for optimization. In this case, we obtain a smaller resolution for deep layers and, consequently, a less accurate inverse model (Figure 11). The inverse model shows reasonable results for the shallow part of the subsurface, but less than 30 m, the inversion suggests a water-saturated formation that was not confirmed by ERT and borehole data.

Figure 12 shows that the measured amplitude and relaxation time are equally well fitted by both inverse models. However, a better fit of the phase is provided by the inversion of complex signals, considering the frequency offset derived from MRS measurements.

DISCUSSION

We have shown that the equivalence problem requires knowledge of the cause of the Larmor frequency variations (time or depth) and, thus, understanding of the behavior of the earth's magnetic field is an important issue for inversion.

In practice, a time-varying GMF is a rather common case that is easily identified. Derivation of the frequency offset is straightforward from measured signals, and this information can be used for forward modeling. This case was tested with synthetic and real data and can be recommended for users. Note that some imprecision may be caused by a rapidly varying GMF during stacking. To avoid this, one should record the GMF on surface with a magnetometer during the measuring interval and then perform a stacking applying correction for the frequency offset. Usually, the GMF varies rather smoothly, and in fact, we did not use such a correction.

A depth-varying GMF is a more complex case, because different layers produce signals with different frequency offsets requiring more complex forward modeling. Data on variations of the earth's magnetic field in the subsurface are not easily available. For example, measurements with a magnetometer on the surface provide only general ideas about the earth's magnetic field in rocks. Measurements in boreholes are not always available and moreover they are localized around the borehole. The frequency-offset distribution necessary for forward modeling can be obtained through a nonlinear inversion of MRS signals, but a 1D model of the GMF in rocks is not always easy to justify; 3D inversion for the frequency offset requires a more complex measuring setup and a more advanced inversion procedure. However, we have developed and tested a 1D inversion algorithm that allows considering a depth-varying frequency offset. Using synthetic data, we were able to recover the initial model. For experimental verification of this algorithm, however, we faced a serious difficulty in finding a place with a known GMF distribution in the subsurface. Thus, we consider that our approach may be

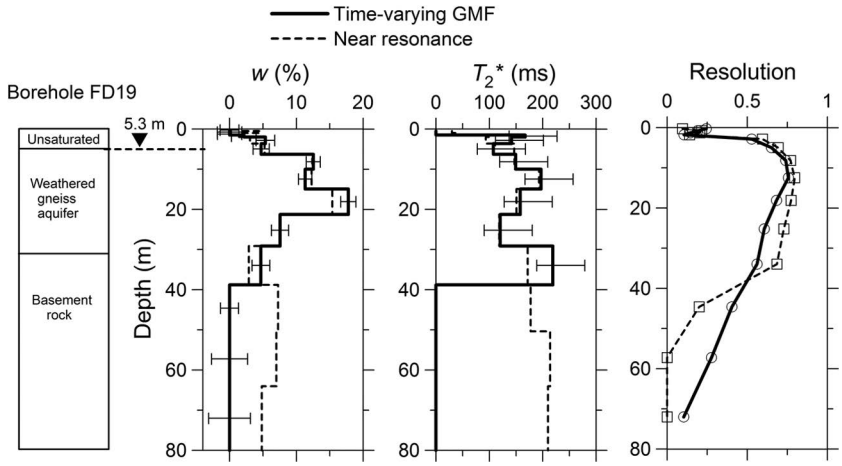

Figure 11. MRS results in Benin (18/09/2014). MRS inversion was carried out using a measured time-varying frequency offset corresponding to a time-varying GMF (solid line). For comparison, the same data set was inverted assuming near-resonance conditions (dashed line). The uncertainty corresponding to the inversion with the near-resonance forward model is defined by the regularization and is similar to that for the time-varying GMF.

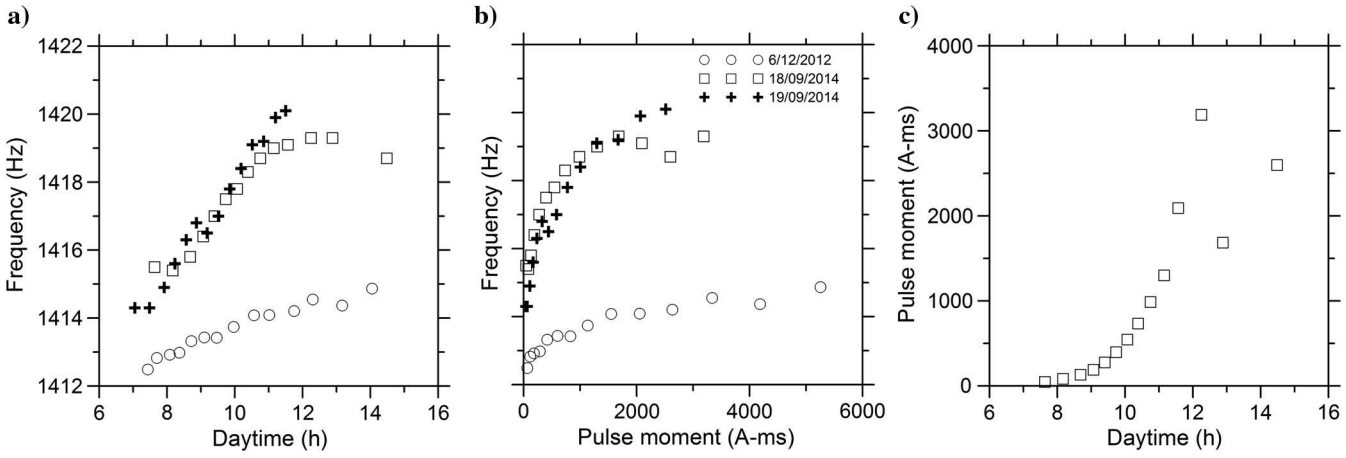

Figure 10. Observed variations in the GMF in Benin carried out during MRS measurements (converted into frequency): (a) time monitoring of the GMF with a proton magnetometer on the surface, (b) corresponding frequency of the MRS signal versus pulse moment, and (c) pulse moment and corresponding daytime of realization.

promising for cases in which the earth's magnetic field in the subsurface shows relatively small variations. In the future, more efforts should be made for testing and rendering such processing more sophisticated.

Awaiting further developments, we thus propose a practical procedure for measuring and interpreting MRS data in a varying GMF (Figure 13).

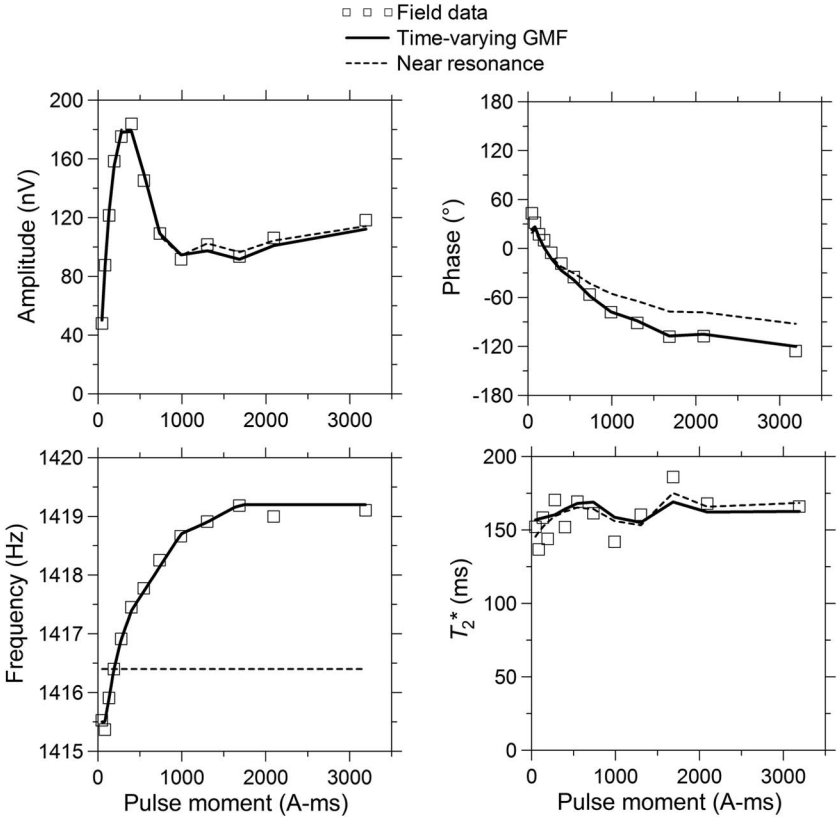

Figure 12. Experimental data set and inversion fit corresponding to the inverse models are shown in Figure 11.

Fieldwork	Interpretation	
◆ Check the Larmor frequency of MRS signal before starting sounding and set the exact frequency ◆ Make GMF measurements during the sounding using a magnetometer ◆ After sounding is done repeat MRS signal measurement for one or more *Q* values separated in time ◆ Change the order of *Q* values in the sounding	***Constant frequency offset***	Compute the linear filter with the constant frequency offset measured with the MRS system
	Time-varying frequency offset	Compute MRS signal considering measured frequency offset for each *Q* value and adjust inversion within the data uncertainty
	Depth-varying frequency offset	Inversion of the Larmor frequency with the Z-varying frequency assumption

Figure 13. Recommended measuring and interpretation procedures when expecting a varying earth's magnetic field and, consequently, a varying frequency offset.

CONCLUSION

We have shown that inversion of MRS data can be improved by taking into account variations of the earth's magnetic field (GMF). The GMF may vary over time and with depth, and it is important to know the origin of these variations.

Although considering a time-varying GMF is straightforward, a depth-varying GMF requires nonlinear inversion of MRS measurements. We developed and successfully tested on synthetic data an algorithm for 1D inversion of MRS data, but this approach still requires practical verification.

We propose a simple procedure for measuring and interpretation of MRS data, considering possible variations in the earth's magnetic field.

ACKNOWLEDGMENTS

The authors acknowledge financial support provided by the French National Program (ANR) Investment for Future — Excellency Equipment project EQUIPEX CRITEX (grant # ANR-11-EQPX-0011). Field data in Benin were obtained as part of the Groundwater Resources in Basement rocks of Africa project funded by the African Union, the European Union, and the French Institut de Recherche pour le Développement (grant AURG/098/2012). This work also benefited from the support of the AQUI BENIN JEAI project funded by IRD. The content of this paper is the sole responsibility of the authors and can under no circumstance be regarded as reflecting the position of the European Union or the African Union.

REFERENCES

Behroozmand, A., E. Auken, G. Fiandaca, and A. V. Christiansen, 2012, Improvement in MRS parameter estimation by joint and laterally constrained inversion of MRS and TEM data: Geophysics, **77**, no. 4, WB191–WB200, doi: 10.1190/geo2011-0404.1.

Braun, M., M. Hertrich, and U. Yaramanci, 2005, Study on complex inversion of magnetic resonance sounding signals: Near Surface Geophysics, **3**, 155–163, doi: 10.3997/1873-0604.2005011.

Braun, M., and U. Yaramanci, 2008, Inversion of resistivity in magnetic resonance sounding: Journal of Applied Geophysics, **66**, 151–164, doi: 10.1016/j.jappgeo.2007.12.004.

Hertrich, M., 2008, Imaging of groundwater with nuclear magnetic resonance: Progress in Nuclear Magnetic Resonance Spectroscopy, **53**, 227–248, doi: 10.1016/j.pnmrs.2008.01.002.

Legchenko, A. V., 2004, Magnetic resonance sounding: Enhanced modeling of a phase shift: Applied Magnetic Resonance, **25**, 621–636, doi: 10.1007/BF03166553.

Legchenko, A. V., 2013, Magnetic resonance imaging for groundwater: Wiley-ISTE.

Legchenko, A. V., A. Beauce, A. Guillen, P. Valla, and J. Bernard, 1997, Natural variations in the magnetic resonance signal used in PMR groundwater prospecting from the surface: European Journal of Environmental and Engineering Geophysics, **2**, 173–190.

Legchenko, A. V., M. Ezersky, J. F. Girard, J. M. Baltassat, M. Boucher, C. Camerlynck, and A. Al-Zoubi, 2008, Interpretation of magnetic resonance soundings in rocks with high electrical conductivity:

Journal of Applied Geophysics, **66**, 118–127, doi: 10.1016/j.jappgeo.2008.04.002.
Legchenko, A. V., and G. Pierrat, 2014, Glimpse into the design of MRS instrument: Near Surface Geophysics, **12**, 297–308, doi: 10.3997/1873-0604.2014006.
Legchenko, A. V., and O. A. Shushakov, 1998, Inversion of surface NMR data: Geophysics, **63**, 75–84, doi: 10.1190/1.1444329.
Legchenko, A. V., and P. Valla, 2002, A review of the basic principles for proton magnetic resonance sounding measurements: Journal of Applied Geophysics, **50**, 3–19, doi: 10.1016/S0926-9851(02)00127-1.
Legchenko, A. V., J. M. Vouillamoz, and J. Roy, 2010, Application of the magnetic resonance sounding method to the investigation of aquifers in the presence of magnetic materials: Geophysics, **75**, no. 6, L91–L100, doi: 10.1190/1.3494596.
Mansfield, P., A. A. Maudsley, P. G. Morris, and I. L. Pykett, 1979, Selective pulses in NMR imaging: Replay to criticism: Journal of Magnetic Resonance, **33**, 261–274.
Marquardt, D., 1963, An algorithm for least-squares estimation of non-linear parameters: Journal of the Society for Industrial and Applied Mathematics, **11**, 431–441, doi: 10.1137/0111030.
Mohnke, O., and U. Yaramanci, 2002, Smooth and block inversion of surface NMR amplitudes and decay times using simulated annealing: Journal of Applied Geophysics, **50**, 163–177, doi: 10.1016/S0926-9851(02)00137-4.
Mohnke, O., and U. Yaramanci, 2005, Forward modeling and inversion of MRS relaxation signals using multiexponential decomposition: Near Surface Geophysics, **3**, 165–185, doi: 10.3997/1873-0604.2005012.
Mueller-Petke, M., and U. Yaramanci, 2010, QT-inversion-comprehensive use of the complete surface-NMR data set: Geophysics, **75**, no. 4, WA199–WA209, doi: 10.1190/1.3471523.
Roy, J., A. Rouleau, M. Chouteau, and M. Bureau, 2008, Widespread occurrence of aquifers currently undetectable with the MRS technique in the Grenville geological province, Canada: Journal of Applied Geophysics, **66**, 82–93, doi: 10.1016/j.jappgeo.2008.04.006.
Vouillamoz, J. M., M. Descloitres, J. Bernard, P. Fourcassié, and L. Romagny, 2002, Application of integrated magnetic resonance sounding and resistivity methods for borehole implementation: A case study in Cambodia: Journal of Applied Geophysics, **50**, 67–81, doi: 10.1016/S0926-9851(02)00130-1.
Vouillamoz, J. M., G. Favreau, S. Massuel, M. Boucher, Y. Nazoumou, and A. Legchenko, 2008, Contribution of magnetic resonance sounding to aquifer characterization and recharge estimate in semiarid Niger: Journal of Applied Geophysics, **64**, 99–108, doi: 10.1016/j.jappgeo.2007.12.006.
Vouillamoz, J. M., A. Legchenko, Y. Albouy, M. Bakalowicz, J. M. Baltassat, and W. Al-Fares, 2003, Localization of saturated karst aquifer with magnetic resonance sounding and resistivity imagery: Journal of Ground Water, **41**, 578–586, doi: 10.1111/j.1745-6584.2003.tb02396.x.
Vouillamoz, J. M., A. Legchenko, and L. Nandagiri, 2011, Characterizing aquifers when using magnetic resonance sounding in a heterogeneous geomagnetic field: Near Surface Geophysics, **9**, 135–144, doi: 10.3997/1873-0604.2010053.
Walbrecker, J. O., M. Hertrich, and A. G. Green, 2011, Off-resonance effects in surface nuclear magnetic resonance: Geophysics, **76**, no. 2, G1–G12, doi: 10.1190/1.3535414.
Weichman, P. B., D. R. Lun, M. H. Ritzwoller, and E. M. Lavely, 2002, Study of surface nuclear magnetic resonance inverse problems: Journal of Applied Geophysics, **50**, 129–147, doi: 10.1016/S0926-9851(02)00135-0.